

Theoretical study of the implications of causality when inferring metamaterial properties

A. Eugene DePrince III and Stephen K. Gray
gray@anl.gov

Center for Nanoscale Materials, Argonne National Laboratory, Argonne, IL 60439

Abstract: The usual procedures to extract effective refractive indices for negative-index metamaterials are complicated by branching ambiguities in the inverse cosine function. The existing methods to eliminate ambiguities either involve calculations with varying geometries which are inherently flawed, as metamaterial properties depend strongly on geometry, or are more subjective as one must inspect and select branches to yield effective parameters as a continuous function of frequency. We propose that the Kramers-Kronig relations, which hold for negative-index materials, naturally guide the selection of the proper branches, and in fact predict negative refractive index where other extraction procedures alone might not. The experimental realization of high quality negative-index materials requires a robust and reliable index retrieval procedure; the combined extraction/Kramers-Kronig retrieval can be used to design optimal metamaterials in a simple, systematic, and general manner.

© 2018 Optical Society of America

OCIS codes: (160.3918) Metamaterials; (160.4236) Nanomaterials; (160.4760) Optical properties; (160.4670) Optical materials

References and links

1. V. G. Veselago, "The electrodynamics of substances with simultaneously negative ϵ and μ ," *Sov. Phys. Usp.* **10**, 509 (1968).
2. J. B. Pendry, "Negative refraction makes a perfect lense," *Phys. Rev. Lett.* **85**, 3966 (2000).
3. D. R. Smith, W. J. Padilla, D. C. Vier, S. C. Nemat-Nasser, and S. Schultz, "Composite medium with simultaneously negative permeability and permittivity," *Phys. Rev. Lett.* **84**, 4184 (2000).
4. D. R. Smith and N. Kroll, "Negative refractive index in left-handed materials," *Phys. Rev. Lett.* **85**, 2933 (2000).
5. V. M. Shalaev, W. Cai, U. K. Chettiar, H.-K. Yuan, A. K. Sarychev, V. P. Drachev, and A. V. Kildishev, "Negative index of refraction in optical metamaterials," *Opt. Lett.* **30** 3356 (2005).
6. R. A. Depine, and A. Lakhtakia, "A new condition to identify isotropic dielectric-magnetic materials displaying negative phase velocity," *Microwave Opt. Tech. Lett.* **2004**, 41, 315.
7. A. Berrier, M. Mulot, M. Swillo, M. Qiu, L. Thylen, A. Talneau, and S. Anand, "Negative refraction at infrared wavelengths in a two-dimensional photonic crystal," *Phys. Rev. Lett.* **93**, 073902 (2004).
8. E. Schonbrun, M. Tinker, W. Park, and J.-B. Lee, "Negative refraction in a Si-polymer photonic crystal membrane," *IEEE Photon. Tech. Lett.* **17**, 1196 (2005).
9. X. Wang and K. Kempa, "Effects of disorder on subwavelength lensing in two-dimensional photonic crystal slabs," *Phys. Rev. B* **71**, 085101 (2005).
10. D.R. Smith, D. Schurig, M. Rosenbluth, S. Schultz, S.A. Ramakrishna, and J.B. Pendry, "Limitations on subdiffraction imaging with a negative index slab," *Appl. Phys. Lett.* **82**, 1506 (2003).
11. C. Luo, S.G. Johnson, J.D. Joannopoulos, and J.B. Pendry, "Subwavelength imaging in photonic crystals," *Phys. Rev. B.* **68**, 045115 (2003).
12. R.A. Shelby, D.R. Smith, S.C. Nemat-Nasser, and S. Schultz, "Microwave transmission through a two-dimensional, isotropic, left-handed material," *Appl. Phys. Lett.* **78**, 489 (2001).

13. J.B. Pendry, A.J. Holden, W.J. Stewart, and I. Youngs, "Extremely low frequency plasmons in metallic mesostructures," *Phys. Rev. Lett.* **76**, 4773 (1996).
 14. J. B. Pendry, A. J. Holden, D. J. Robbins, and W. J. Stewart, "Magnetism from conductors and enhanced nonlinear phenomena," *IEEE Trans. Microwave Theor. Tech.* **47**, 2057 (1999).
 15. R. A. Shelby, D. R. Smith, and S. Schultz, "Experimental verification of a negative index of refraction," *Science* **292**, 77 (2001).
 16. P. Markos and C.M. Soukoulis, "Transmission properties and effective electromagnetic properties of double negative materials," *Optics Express* **11** 649 (2003).
 17. C. Enkrich, M. Wegener, S. Linde, S. Burger, L. Zschiedrich, F. Schmidt, J.F. Zhou, T. Koschny, and C.M. Soukoulis, "Magnetic metamaterials at telecommunication and visible frequencies," *Phys. Rev. Lett.* **95**, 203901 (2005).
 18. T. A. Klar, A. V. Kildishev, V. P. Drachev, and V. M. Shalaev, "Negative-Index Metamaterials: Going Optical," *IEEE J. Sel. Top. Quant. Elec.* **12**, 1106 (2006).
 19. V. P. Drachev, W. Cai, U. Chettiar, H.-K. Yuan, A. K. Sarychev, A. V. Kildishev, G. Klimeck, and V. M. Shalaev, "Experimental verification of an optical negative-index material," *Laser Phys. Lett.* **3**, 49 (2006).
 20. A. V. Kildishev, W. Cai, Y. K. Chettiar, H.-K. Yuan, A. K. Sarychev, V. P. Drachev, and V. M. Shalaev, "Negative refractive index in optics of metal-dielectric composites," *J. Opt. Soc. Am. B* **23**, 423 (2006).
 21. H. Chen, L. Ran, J. Huangfu, X. Zhang, and K. Chen, "Left-handed materials composed of only S-shaped resonators," *Phys. Rev. E* **70**, 057605 (2004).
 22. D. Wang, L. Ran, H. Chen, M. Mu, J.A. Kong, and B.-I. Wu, "Experimental validation of negative refraction of metamaterial composed of single side paired S-ring resonators," *Appl. Phys. Lett.* **90**, 254103 (2007).
 23. S.N. Burokur, T. Lepetit, and A. de Lustrac, "Incidence dependence of negative index in asymmetric cut wire pairs metamaterials," *Appl. Phys. Lett.* **95** 191114 (2009).
 24. D. R. Smith, S. Schultz, P. Markos, and C. M. Soukoulis, "Determination of effective permittivity and permeability of metamaterials from reflection and transmission coefficients," *Phys. Rev. B* **65**, 195104 (2002).
 25. D. R. Smith, D. C. Vier, Th. Koschny, and C. M. Soukoulis, "Electromagnetic parameter retrieval from inhomogeneous metamaterials," *Phys. Rev. E* **71** 036617 (2005).
 26. X. Chen, T.M. Grzegorzczak, B.-I. Wu, J. Pacheco, Jr., and J.A. Kong, "Robust method to retrieve the constitutive effective parameters of metamaterials," *Phys. Rev. E* **70**, 016608 (2004).
 27. A.F. Oskooi, D. Roundy, M. Ibanescu, P. Bermel, J.D. Joannopoulos, S.G. Johnson, "Meep: A flexible free-software package for electromagnetic simulations by the FDTD method," *Comput. Phys. Comm.* **181**, 687 (2010).
 28. M. Altarelli, D. L. Dexter, H. M. Nussenzveig, and D. Y. Smith, "Superconvergence and sum rules for the optical constant," *Phys. Rev. B* **6**, 4502 (1972).
 29. K.-E. Peiponen, V. Lucarini, E. M. Vartiainen, and J. J. Saarinen, "Kramers-Kronig relations and sum rules of negative refractive index media," *Eur. Phys. J. B* **41**, 61 (2004).
 30. J. Skaar, "Fresnel equations and the refractive index of active media," *Phys. Rev. E* **73**, 026605 (2006).
 31. M. I. Stockman, "Criterion for negative refraction with low optical losses from a fundamental principle of causality," *Phys. Rev. Lett.* **98**, 177404 (2007).
-

1. Introduction

Artificial materials known as metamaterials can exhibit a range of unique electromagnetic properties that are not observed in naturally occurring materials. Obtaining a negative index of refraction is particularly desirable, as negative-index materials (NIM) have many potential applications including imaging beyond the diffraction limit and optical cloaking. Although NIM were characterized by Veselago [1] many years ago, it is only recently that we have seen a sudden burst in interest in NIM design and applications. Pendry [2] showed that perfect subwavelength imaging or superlensing would be possible with a NIM of refractive index $N = -1 + 0i$. The exciting idea here is that imaging would be limited not by the wavelength of light, but by the quality of the lense. Double negative materials and NIM were shortly thereafter experimentally realized in the work of Smith and coworkers [3, 4]. In addition, the functional range of NIM has been driven to visible frequencies by Shalaev by incorporating the visible-range electromagnetic resonances of metallic nanoparticles into NIM design [5]. In practice, sufficient conditions to yield a negative refractive index come in the form of $\text{Re}(\epsilon) < 0, \text{Re}(\mu) < 0$, where ϵ and μ represent the relative permittivity and permeability of the material, respectively. Materials having simultaneously negative permeability and permittivity are known as double negative materials. Note, however, that these conditions are sufficient but not necessary to achieve a

negative index. Necessary conditions require only that $\text{Re}(\epsilon)\text{Im}(\mu) + \text{Im}(\epsilon)\text{Re}(\mu) < 0$ [6].

Several classes of NIM have been realized experimentally with a few standard designs emerging that yield negative indices in a wide range of frequencies. Photonic crystals [7, 8, 9] have been shown to exhibit a negative index in the near-IR range, but their utility as imaging devices is limited by the internal structure of the crystal, which has dimensions on the order of the wavelength of light [10, 11]. Split-ring resonators (SRR) [12, 13, 14, 15, 16, 17] can exhibit negative index at telecommunication wavelengths. In general, the SRR provides a negative permeability that, when combined with the negative permittivity of a metallic component, results in a negative real component of the refractive index. The operating frequencies of the SRR can be shifted toward the visible range by miniaturization. The first class of NIM to reach the visible spectrum is perhaps the simplest and in that sense the most versatile. A pair of nanowires separated by some dielectric has been shown theoretically and experimentally give a negative refractive index in the near IR and visible range [5, 18, 19, 20]. There also exist S-shaped variations on the wire-pair structure in the spirit of the SRR known as S-shaped resonators [21, 22]. The behavior of double S-shaped resonators can be mimicked by a single pair of asymmetric parallel nanowires [23], which bear strong resemblance to the simple metal-dielectric-metal sandwich described above.

Clearly there exist many possibilities for high quality NIM, and characterizing the refractive index theoretically can aid the design of such materials, circumventing the need for expensive experimental optimizations of metamaterial geometries. Refractive index retrieval methods based on scattering- or S-parameters [16, 24, 25, 26] are the most direct and robust methods for relating refractive index to theoretically and experimentally tractable parameters such as complex transmission and reflection coefficients. The extraction procedures work reasonably well in most cases, but, occasionally, severe branching ambiguities muddle the procedure and introduce an element of subjectivity into the index assignments. In this paper, we suggest a simple and powerful method for automatically selecting the correct branches in the extraction procedure by invoking the concept of causality. The well-known Kramers-Kronig relations automatically guide the extraction procedure and in some cases allow us to predict a structure to be a NIM that would otherwise be difficult to characterize.

2. Theory

S-parameter retrieval procedures begin with the assumption that the metamaterial may be approximated by a homogeneous slab with a well-defined thickness, D . The complex transmission and reflection coefficients are given by [5]

$$t = e^{ik(D-2\delta)} \frac{E_t(\delta)}{E_i(-\delta)}, \quad (1)$$

and

$$r = e^{ik(D-2\delta)} \frac{E_r(-\delta)}{E_i(-\delta)}, \quad (2)$$

where δ is the distance from the center of the slab to the evaluation planes above and below the sample. The reflected and transmitted fields are normalized by the incident light, E_i at the reflection evaluation plane. The refractive index for a homogeneous NIM in vacuum (or on a substrate with refractive index equal to unity) is given by

$$N = \pm \frac{1}{kD} \cos^{-1} \left(\frac{1 - r^2 + t^2}{2t} \right) + \frac{2m\pi}{kD}. \quad (3)$$

The sign in Eq. (3) is uniquely determined by requiring that $\text{Im}(N)$ be positive. However, the real portion of the inverse cosine function is prone to branching ambiguities, where seemingly

valid solutions exist for all integers, m . The S-parameter retrieval is based in the assumption that the metamaterial may be treated as a homogeneous material, and as such, the macroscopic refractive index should be independent of the thickness of the NIM, D . To maximize the separation of the branches, the extraction procedure should be performed on as thin a slab as possible, and even then, one should perform more than one analysis with differing values for D . The true branches should reveal themselves in their insensitivity to the choice of D . Unfortunately, metamaterial properties are very sensitive to geometric parameters, and it is virtually impossible to alter D in such a way as to maintain a constant refractive index. Choosing branches becomes a more subjective process wherein one selects parameters as a continuous function of frequency [16, 24]. We will show that this process is still flawed, as the solution can be skewed by spurious discontinuities in the refractive index as a function of frequency.

The ambiguities in the extraction procedure are ultimately rooted in (and may ultimately be circumvented by) the fact that Eq. (3) is insufficient to guarantee that the obtained refractive indices are causal; that is, do the real and imaginary components reflect the analytical properties of ϵ and μ ? The well-known Kramers-Kronig (KK) relations [28, 29] guarantee that knowledge of the imaginary component of the refractive index over all frequencies implies knowledge of the real component by the integration

$$n(\omega) - n_\infty = \frac{2}{\pi} \text{P} \int_0^\infty \frac{\omega' \kappa(\omega')}{\omega'^2 - \omega^2} d\omega'. \quad (4)$$

Similarly, knowledge of the real component over all frequencies can be mapped to the imaginary component:

$$\kappa(\omega) = -\frac{2\omega}{\pi} \text{P} \int_0^\infty \frac{n(\omega') - n_\infty}{\omega'^2 - \omega^2} d\omega'. \quad (5)$$

Regardless of the extent to which branching issues complicate the extraction procedure, the KK relationship between the real and imaginary components of the refractive index must hold at all wavelengths. The correct form of $\text{Im}(N)$ is easy to obtain from Eq. (3); one simply selects the sign such that the imaginary component is positive. We can verify the validity of the similarly obtained real components by integrating Eq. (4) over frequencies that effectively span the range 0 to ∞ . In practice, very accurate values for $\text{Re}(N)$ may be obtained by numerically integrating Eq. (4) over a very wide, finite range of frequencies. The infinite-frequency limit of the refractive index, n_∞ , is given by the extraction procedure in the limit of very small wavelength. In the limit of $\omega \rightarrow \infty$, all branches in the inverse cosine function converge and all ambiguities are removed.

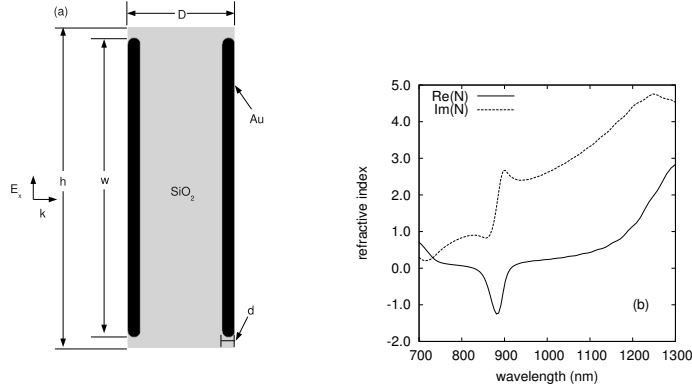
It should be noted that we have used Kramers-Kronig relations concerning $N = n + i\kappa$. Somewhat less convenient for our purposes, but more fundamental, KK relations exist for ϵ and μ . The validity of our KK relations requires that N be analytic in the upper half of the complex plane, $N \rightarrow n_\infty$ as $\omega \rightarrow \infty$, and no conductivity at $\omega = 0$. These conditions in relation to metamaterials were discussed by Skaar [30]. In particular, the metamaterial must be a passive medium, with no gain. However, it has also been pointed out that N^2 has the same analytical properties as ϵ and μ separately, and therefore a KK relation for N^2 would be appropriate in the case of gain [31]. We have verified numerically that the computed n and κ from our approach discussed below satisfy this other KK relation. In future work, it may be interesting to consider the use of this relation directly.

3. Applications

We consider a two-dimensional system of gold nanorods separated by SiO_2 similar to that investigated by Shalaev *et al.* [20]. The system is illustrated in Fig. 1(a), with the parameters given in Ref. [20] to obtain negative refractive index; the rods of thickness $d=13$ nm and width

$w=450$ nm are separated by SiO_2 with a total slab thickness of $D=160$ nm. The system is periodic in the x -direction with a periodicity of $h=480$ nm. We obtain the complex transmission and reflection coefficients with finite-difference time-domain (FDTD) simulations as implemented in the freely available Meep FDTD package [27]. This particular structure, as noted in Ref [20] and depicted in Fig 1(b), clearly exhibits a negative refractive index in the 850-900 nm region. Our present results reproduce well those given in Ref. [20]. As an aside, we note that the per-

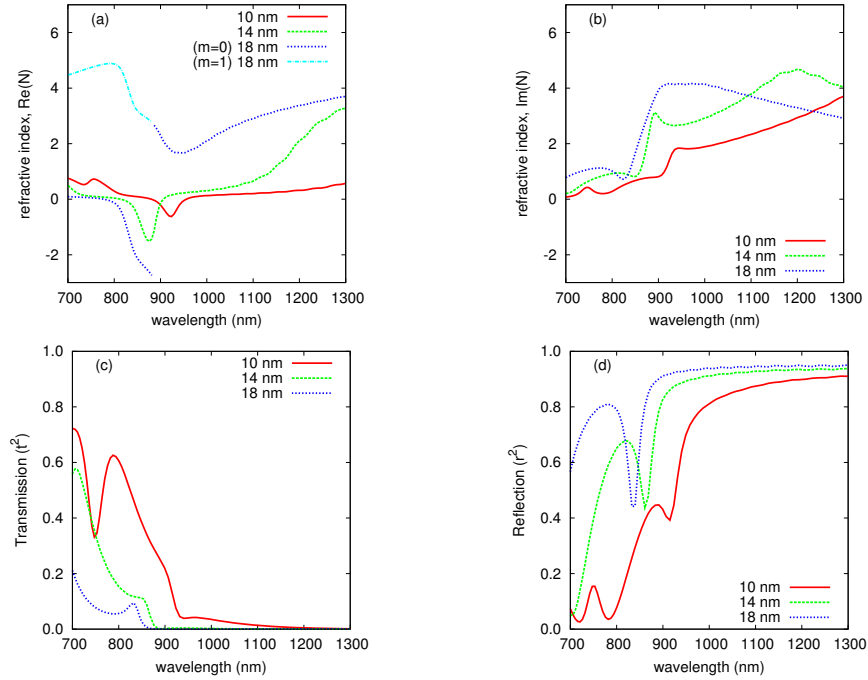
Fig. 1. The unit cell of a two-dimensional NIM composed of two Au rods separated by SiO_2 (a). The real component of the refractive index (b) is clearly negative in the 850-900 nm range.



meability for this structure is positive; the structure is a NIM but *not* a double negative material. The material does, however, satisfy the necessary conditions given in Ref. [6]. Optimizing this structure for negative real component of the refractive index, we consider first only varying the rod thickness, d , while holding all parameters at their values listed above. Figure 2 illustrates the real and imaginary components of the refractive index obtained from the extraction in Eq. (3) as well as transmission and reflection spectra. The real component of the refractive index for the $d = 10$ and $d = 14$ nm cases (Fig. 2(a)), like the $d = 13$ nm case, is unambiguously determined by the extraction procedure. However, a discontinuity develops in the $m=0$ branch for $d = 18$ nm. As stated above, the macroscopic refractive index should be independent of slab thickness, and this property should be exploited in assigning branches. In practice, though, a NIM almost never exhibits this nice property, and the assignment must be made on the basis of maintaining the continuity of the refractive index as a function of frequency. A continuous refractive index function can be obtained for $d = 18$ nm by combining the $m=0$ and $m=1$ branches, resulting in the upper continuous curve. However, this choice gives the refractive index as a discontinuous function of the rod thickness, d . One would expect that such an abrupt change in character of the refractive index would be associated with an equally abrupt change in either the imaginary component of the refractive index or the transmission or reflection spectra, but each of these do indeed vary smoothly with the geometric parameter, d . The imaginary component of the refractive index does lose a sharp peak when increasing d from 14 to 18 nm, but this change is subtle compared to that suggested by Fig. 2(a). We propose that the correct form of $\text{Re}(N)$ may be obtained unambiguously by the integration of $\text{Im}(N)$ according to Eq. (4).

Consider again the well-behaved system ($d=13$ nm) in which negative refractive index is observed in the 850-900 nm range. The values for the index extracted from Eq. (3) and those obtained by integration of Eq. (4) should be equivalent, provided that we have integrated $\text{Im}(N)$

Fig. 2. Real (a) and imaginary (b) components of the refractive index extracted according to Eq. (3) as well as transmission (c) and reflection (d) spectra for various rod thicknesses, d. All other parameters are held constant at the values detailed in the text.



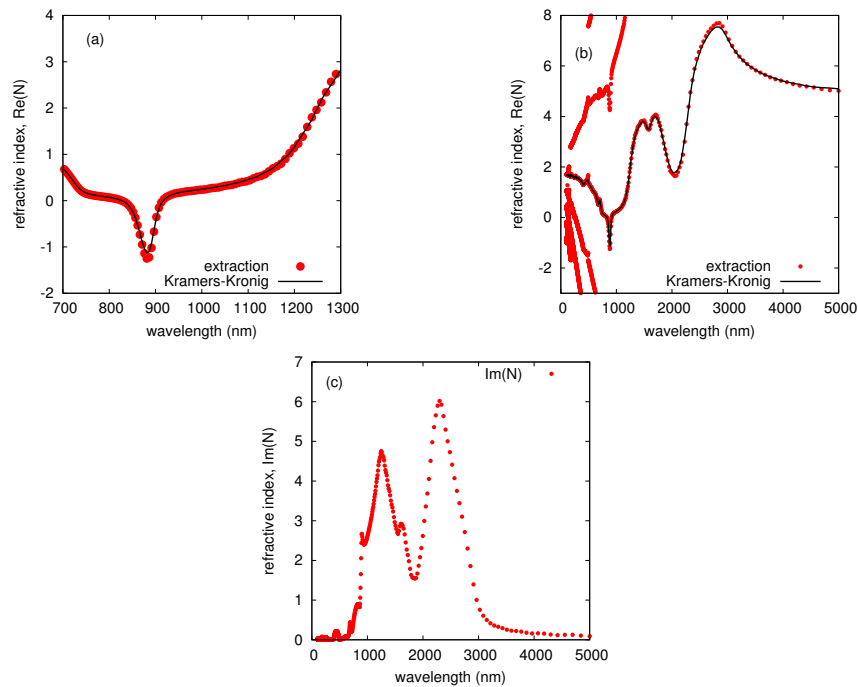
over an appropriately large range of frequencies. Table 1 lists the non-parallelity errors (NPE) obtained for $\text{Re}(N)$ obtained from the KK integration as compared to that obtained from the extraction procedure for several different wavelength ranges. NPE are defined here by taking

Table 1. Non-parallelity error (NPE) in the Kramers-Kronig integration as compared to extracted values of $\text{Re}(N)$. The NPE is defined as the difference between the most positive and most negative errors between the KK and extracted values of $\text{Re}(N)$ over the range 700-1300 nm.

wavelength (nm)		NPE
minimum	maximum	
700	1300	5.434
700	1500	1.224
700	2000	0.742
700	5000	0.478
100	1300	5.071
100	1500	0.862
100	2000	0.380
100	5000	0.200

the difference between the most positive and most negative errors in the KK integration as compared to the extracted values of $\text{Re}(N)$ in the range of 700-1300 nm. Integration over only the range of interest (700-1300 nm) leads to very large errors, and the integrated values of $\text{Re}(N)$ are virtually meaningless. The KK value for $\text{Re}(N)$ become quite accurate when we extend the integration range to 100-5000 nm, as is evidenced by the NPE in Table 1 and visually in Figs. 3(a) and (b). The KK integration reproduces the negative region of refractive index in the

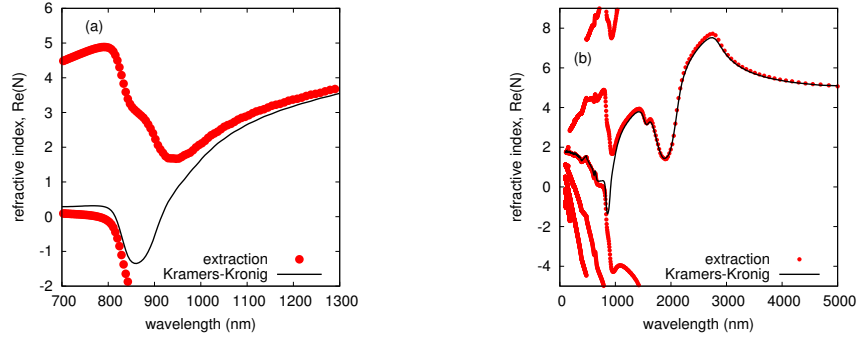
Fig. 3. Real and imaginary components of the refractive index as obtained from the extraction in Eq. (3) and, for the real component, the Kramers-Kronig integration of Eq. (4). Results are presented for a gold nanorod system with $d=13$ nm.



850-900 nm region as well as all other features from 100-5000 nm. The very large and very wide features present in $\text{Im}(N)$ in Fig. 3(c) illustrate the importance of such a wide range of frequencies for obtaining reliable results; these broad features significantly contribute to the KK integral.

Now consider the $d=18$ nm case in which a discontinuity developed in the $m=0$ branch, and the choice for the correct branch is made subjectively. Forcing $\text{Re}(N)$ to be a continuous function of wavelength would require one to combine the $m=0$ and $m=1$ branches to form the upper curve in Fig. 2(a), but as shown in Fig. 4, the correct choice as determined by KK integration involves *only* the $m=0$ branch in the 700-1300 nm range, yielding a negative index with a minimum around 880 nm. The original branch assignment based solely on the extraction procedure and continuity of the refractive index predicts no negative index and is thus qualitatively incorrect. Ambiguous situations such as this where index assignments are based on the continuity of $\text{Re}(N)$ are surprisingly common, and the KK integration can provide a very easy and necessary check as to the validity of branch assignments. The question remains as to *why* the extraction procedure results in a spurious discontinuity in such an important frequency range. In general

Fig. 4. Real component of the refractive index as obtained from the extraction in Eq. (3) or the Kramers-Kronig integration of Eq. (4) for a gold nanorod system with $d=18$ nm.



we observe that, for a gold nanorod NIM of fixed width, D , as the ratio of d to D increases, a false discontinuity inevitably develops in the extracted values of $\text{Re}(N)$. The KK integration, by enforcing causality, can be used to interpolate through these problematic regions and select the proper branches on either side.

The combined extraction/KK procedure for determining refractive indices, in removing ambiguities in branch assignments, allows for a more “black-box” approach to the optimization of NIM for either very negative refractive index or for a NIM quality factor or figure of merit (FOM) related to the ratios of the real and imaginary components of N :

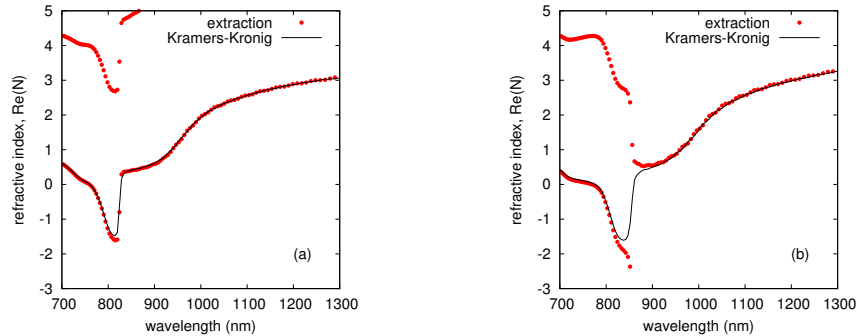
$$\text{FOM} = -\frac{\text{Re}(N)}{\text{Im}(N)}. \quad (6)$$

We have optimized the structure in Fig. 1(a) for the FOM by varying the parameters d , D , and w , sampling a total of 768 structures with d , D , and w in the ranges 12-19 nm, 120-230 nm, and 400-470 nm, respectively. The structure exhibiting the largest FOM as given by Eq. (6) was found to have $d=17$ nm, $D=190$ nm, and $w=430$ nm, with a NIM figure of merit, $\text{FOM} = 1.517$. This value is nearly double the value of 0.829 that corresponds to the structure suggested in Ref. [20] with $d=13$, $D=160$, and $w=450$ nm, and the optimized material is a double negative material, where both μ and ϵ are simultaneously negative. Recall that the $\text{FOM}=0.829$ structure of Ref. [20] has a positive relative permeability. Fourteen structures were found to have figures of merit greater than 1.4, and, surprisingly, four of these structures might not have been found with the simplistic, continuous-function approach to the extraction procedure. Figure 5 depicts the $m=0$ and $m=1$ branches of $\text{Re}(N)$ for the optimal $\text{FOM}=1.517$ as well as the best structure found that exhibits a false discontinuity in the extracted index, with $\text{FOM}=1.442$ ($d = 17$ nm, $D = 180$ nm, $w = 440$ nm). Clearly, the KK relations allow us to easily and unambiguously select the proper branches of $\text{Re}(N)$ obtained from the retrieval. Amazingly, the high-quality structure whose refractive index is represented in Fig. 5(b) would not have been considered a NIM without the KK analysis. This $\text{FOM}=1.442$ structure, like the optimal $\text{FOM}=1.517$ structure, is also a double negative material.

4. Conclusions

We have developed a reliable and robust methodology for extracting effective refractive indices for metamaterials by combining the usual S-parameter extraction procedures with the concept

Fig. 5. Real component of the refractive index as obtained from the extraction in Eq. (3) or the Kramers-Kronig integration of Eq. (4) for a gold nanorod system with (a) FOM=1.517 and (b) FOM=1.442.



of causality as expressed in the Kramers-Kronig relationship. Causality absolutely must be enforced when extracting effective parameters from the three-layer homogenous metamaterial model. Our results suggest that simplistic extraction models in which one copes with branching ambiguities by enforcing continuity of the refractive index as a function of frequency may result in qualitatively incorrect results. In addition, in regions where $\text{Im}(N)$ is very close to zero, the sign chosen for Eq. (3) may suffer from numerical noise; this sign issue has no implications for $\text{Im}(N)$, as it is virtually zero, but $\text{Re}(N)$ may be given the incorrect sign. $\text{Re}(N)$ obtained from KK integration will be insensitive to this issue when $\text{Im}(N)$ is close to zero and will thus yield more reliable results. The Kramers-Kronig relations naturally guide branch selection and are simple enough that they may be used in a “black-box” sense for the optimization of metamaterial geometries for desired properties. The present methodology was used to optimize a gold nanorod system for a NIM quality factor, Q , resulting in a structure with a Q -factor nearly double that of the original starting structure. Several high-quality structures were also obtained that would not have been considered NIM with existing extraction procedures.

The KK relations can also provide a useful gauge as to the validity of the assumption of metamaterial homogeneity that is central to the S-parameter retrieval procedure. One can view the false discontinuities in the refractive index functions as the first symptoms of the breakdown of the validity of the homogeneous three-layer model. In extreme cases, where the amount of metal relative to the dielectric present in the sample becomes significant, the KK relation of Eq. (4) can only qualitatively reproduce the extracted index over the entire frequency spectrum. The KK results are not incorrect; the discrepancy merely reflects the failure of the assumption of the homogeneous nature of the metamaterial. In these rare instances, the extraction procedure as a whole may not be an appropriate way to obtain refractive indices.

5. Acknowledgments

This research used resources of the Argonne Leadership Computing Facility and the Center for Nanoscale Materials at Argonne National Laboratory, which are supported by the Office of Science of the U.S. Department of Energy under contract DE-AC02-06CH11357. AED thanks Jeff Hammond for support on the BlueGene/P system in the Argonne Leadership Computing Facility. We thank Matt Pelton for helpful comments. AED acknowledges funding from the Computational Postdoctoral fellowship through the Computing, Engineering, and Life Sciences

Division of Argonne National Laboratory.